PROC. 19th INT. CONF. HIGH ENERGY PHYSICS
TOKYO, 1978

P 2b Dilepton Production in Hadron Collisions

L. M. LEDERMAN

Columbia University, New York, N.Y. 10027

§I. Introduction

This subject had its inception in a critical letter published in Il Nuovo Cimento in 1966 by one of our hosts, Prof. Y. Yamaguchi.[1] In that paper, he criticized a search for W^+ mesons carried out by a Columbia group.[2] He pointed out that the reaction we were looking at, $pN \to W^+ + X$ would be dominated by a background $pN \to \gamma + X$ in which γ goes to μ pair and in which the effective mass of the virtual photon is equal to that of W^+.

This comment stung us because we had not thought about it at all. (This was also independently pointed out by Okun.[3]) However it also gave us an idea that massive virtual photons could be used as probes for small distance physics. In 1966–67 we designed an experiment for the 30 GeV AGS at Brookhaven, $pN \to \mu^+\mu^- X$.[4]

In our proposal we argued that this was a good way to search for bumps and also to probe small distances.

Figure 1 is then a thumbnail ten year history and summary of my talk after which the reader can skip to the bibliography to see if I have referred to him properly. In 1978 at Tokyo, we have found bumps: J/ψ, ψ' and the Υ family, and what we called, "small distance probe" has become a parton model that successfully correlates all reactions involving leptons and hadrons by virtual photons and W's. That is the optimistic argument I will try to present. I do this grudgingly because it is clearly much more fun to confound the theorists. An outline of this talk follows:

Dilepton Production in Hadron Collisions

Brief History

1968: Columbia-BNL Proposal to Probe Small Distances Using Virtual Photons and to Look for Bumps.

1978: Tokyo

Bumps Have Been Found: J/ψ, ψ', Υ, ...

"Small Distance Probe" Has Found a Constituent (Quark-Gluon) Model Which is Completely Consistent with Lepton Scattering.

Fig. 1.

II. Upsilon Physics
III. Search for New (and Old) Bumps
IV. Dilepton Continuum Physics
  A. Comments on Drell–Yan analysis
  B. Experimental results
  C. Applications of Drell–Yan analysis
  D. Dilepton transverse momenta

Table Ia lists the groups whose data are discussed here together with the dehumanizing acronym that must be used to identify the group. Table Ib gives a resume of the respective experimental parameters.

§II. Upsilon Physics

The CFS group (FNAL), see Fig. 2. There have been four runs:

1) There was the May–August 1977 run of about 1200 upsilons at 400 GeV where the resolution was about 2%, average intensity $\sim 2 \times 10^{11}$ ppp.[5a]

2) September–November 1977 runs at 200 to 300 GeV to get scaling data.[5d] This yielded about 500 upsilons with about the same resolution.

STUDY OF SCALING IN HADRONIC PRODUCTION OF DIMUONS

J.K. Yoh, S.W. Herb, D.C. Hom, L.M. Lederman, J.C. Sens, and H.D. Snyder

Columbia University, New York, N.Y. 10027

and

K. Ueno, B.C. Brown, C.N. Brown, W.R. Innes, R.D. Kephart, and T. Yamanouchi

Fermi National Accelerator Laboratory, Batavia, Ill. 60510

and

R.J. Fisk, A.S. Ito, H. Jöstlein, and D.M. Kaplan

State University of New York, Stony Brook, N.Y. 11974

Fig. 2.

3) November 1977–April 1978 high intensity ($\sim 8 \times 10^{11}$ ppp) at 400 GeV, largely looking for higher mass bumps with a somewhat degraded resolution ($\Delta m/m \sim 2.3\%$).

Table Ia. Principal contributors.

At Fermilab:	
Columbia–Fermilab–Stony Brook	CFS
Seattle–Northeastern–Michigan–Tufts	SNMT
Chicago–Illinois–Princeton	CIP
At ISR:	
CERN–Columbia–Oxford–Rockefeller	CCOR
CERN–Saclay–Zürich	CSZ
(Athens)[2]–CERN–BNL–Syracuse–Yale	ABCSY
CERN–Harvard–Frascati–MIT–Naples–Pisa	CHFMNP
Saclay–Imperial–Southampton–Indiana	SISI

mining the position (in the bending plane) of a point on each trajectory served to improve the resolution from 2.0 to ~1.7%. In order to have this chamber survive, 60 cm of steel was added to our Be absorber and the proton intensity decreased to $\sim 3\times 10^{11}$ ppp. We also obtained some improvement from converting our PWC's to "mini" drift chambers. Figure 5 shows the results of this run with continuum subtracted and one sees the separation of Υ and Υ' now very clearly. As usual Υ'' is indicated by a shoulder on the high

Table Ib. Quality of dilepton data ($\sqrt{s} > 10$, $m \geq 5$).

Group	Reactions	$\sqrt{s}$	$\Delta\sqrt{\tau}$	Δx_F	$\Delta m/m$	No. of events >5 GeV	Assoc. particle capability
CFS	pN	19	0.18–0.65	+0.30→0.60	2%	180,000	No
(Lederman)		23.7		+0.10→0.40			
		27.3		−0.15→+0.75			
SNMT	pN	27.3	0.22–0.60	0.1→0.6	6%	275,000	No
(Garelick)							
ABCSY	pp	52	0.1–0.15	±0.2	4%	~100	Yes
(Willis)		63	0.085–0.16				
CHFMNP	pp	63	0.08–0.24	−0.3 →+0.9	10%	~300	Yes
(Ting–Belletini)							
CCOR	pp	63	0.08–0.22	−0.2 →+0.2	5%	~ 60	Yes
(DiLella)							
CP II	πN	21	0.15–0.50	~ 0 → 1.0	~5%	3,000	No
(Pilcher–Smith)							
SISI	πN	17	0.20–0.60	0 → 0.8	1.5%	~ 80	Yes

About 7,000 upsilons were collected.

4) Finally we turned to higher resolution. Changes in the apparatus yielded a $\Delta m/m$ ~1.5%. About 500 upsilons were collected. These data will appear in various places in the talk.

The data were presented to this conference by T. Yamanouchi.

Figure 3 gives the data from run 1) and Fig. 4 is the result of the long high intensity run 3). The upsilon peak in the new data clearly shows the effects of the poorer resolution, the apparatus suffering under the very high rates (~ 10–20×10^6 ppp). Nevertheless there is data out to ~20 GeV, the upsilon is still there (the good news) but the several intriguing (1–2.5 standard deviation) peaks seen in Fig. 3 have all disappeared from Fig. 4 (see later). In order to improve resolution, we installed a specially designed PWC upstream of the spectrometer magnet[5] in a place where the rates normally exceeded 100 Mcps. Deter-

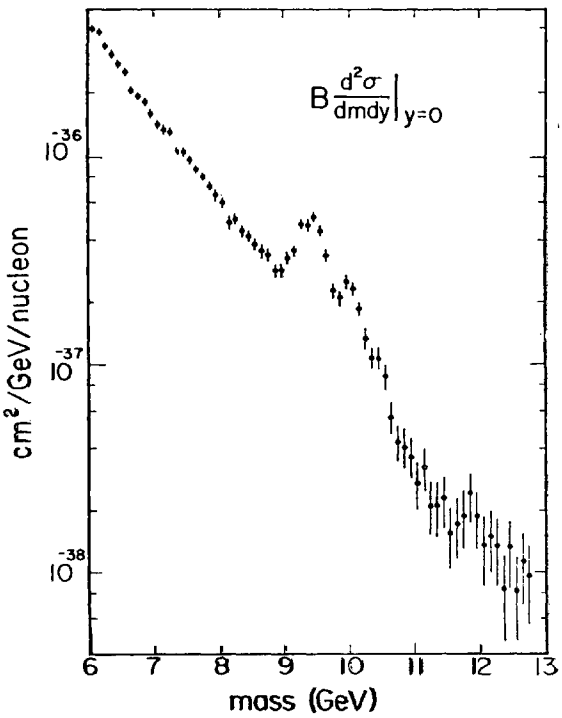

Fig. 3. CFS dimuon data, Summer '75.

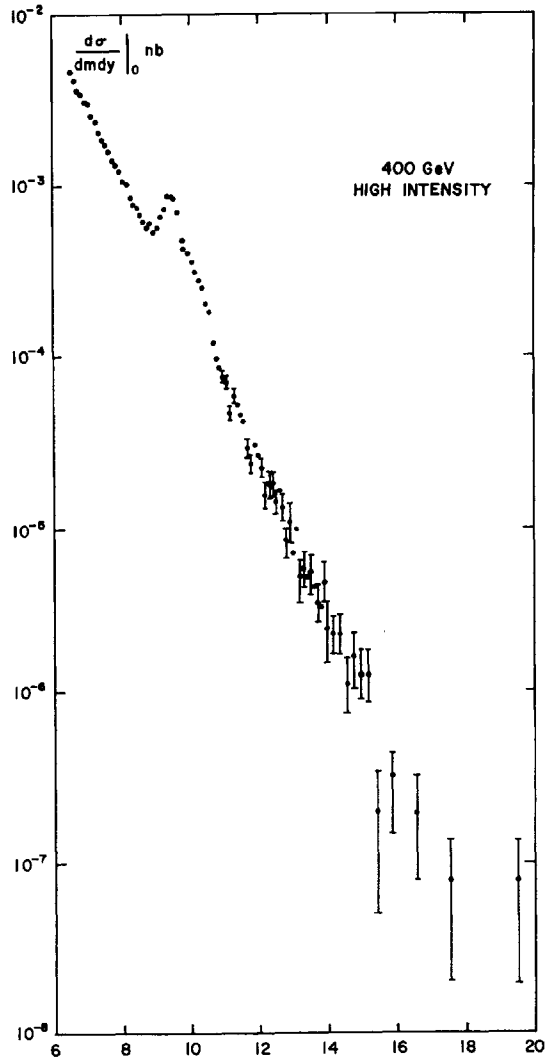

Fig. 4. CFS dimuon data, high intensity.

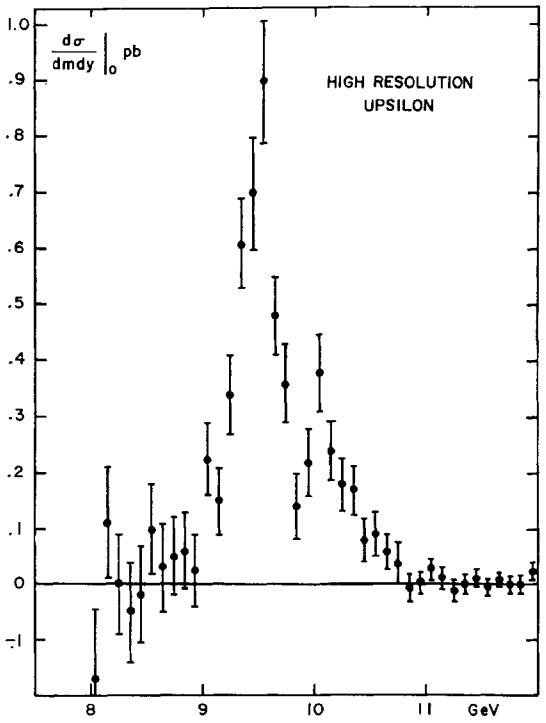

Fig. 5. CFS high resolution upsilon peak with continuum subtracted.

Table II. Upsilon analysis—All data.

	3 Peak Fit	2 Peak Fit
$m(\Upsilon)$	$9.46\pm0.001\pm0.10$	$9.47\pm0.006\pm0.10$
GeV		
$B(d\sigma/dy)(\Upsilon)$	0.27 pb	
$(d^2\sigma/dm\cdot dy)$ (cont.)	0.96 ± 0.03 GeV	1.02 ± 0.03 GeV
$m(\Upsilon')-m(\Upsilon)$	0.590 ± 0.035	0.709 ± 0.012
GeV	$m(\Upsilon')=10.05$	10.18
$\frac{B(d\sigma/dy)(\Upsilon')}{B(d\sigma/dy)(\Upsilon)}$	0.31 ± 0.03	0.35 ± 0.015
$m(\Upsilon'')-m(\Upsilon)$	0.96 ± 0.06	—
GeV	$m(\Upsilon'')=10.42$	
$\frac{B(d\sigma/dy)(\Upsilon'')}{B(d\sigma/dy)(\Upsilon')}$	0.16 ± 0.04	—
χ^2/DF	213/225	247/227
Comment:	Υ'' is $\sim 4\sigma$	

side of the Υ'. Table II shows the result of an analysis that was carried out using *all* of our data. We note that there are strong correlations between the strength of the third peak and the spacing between Υ and Υ'. If we insist there is *no* third peak, the fitting program increases $\Delta m(\Upsilon-\Upsilon')$ from 590 MeV to 709 MeV. Note that the χ^2/DOF increases, the Υ'' being favored by $\sim 4\sigma$. Several days ago, the DESY groups reported the observation of Υ' in e^+e^- collisions.[6] Their mass splitting is: 555 ± 3 or 557 ± 5 MeV.* This splitting was imposed upon the CFS analysis program (*via* telephone) and the result is presented in Table III. Note that under *this* assumption, the Υ'' becomes a 13σ effect. So we have (at least) three narrow peaks. There is another way to designate the upsilon family, which has certain advantages in Japan: Υ, Υ, Υ.

* Newer DESY data (Bienlein *et al.*, DESY 78/45) gives $\Delta m=560\pm10$ MeV.

The SNMT group at FNAL, see Fig. 6. This was described to us by P. Mockett as a forward spectrometer based on magnetized iron deflection of muons. It is a very high statistics experiment; with a large x_F acceptance but obtained at the expense of resolution. Figures 7a, b show their data. When one subtracts a continuum fit (7b), one sees a substantial Υ peak representing the entire, unresolved Υ family. The signal to continuum is in good agreement with CFS in spite of the large x_F acceptance.

Table III. p_T fit parameters.[a,b]

	$\sqrt{s}$ (GeV)	19.4	
	C		p_0
M	(fb. GeV^{-2})		(GeV)
4.5	7169±208		2.07±0.049
5.5	1592± 59		2.34±.055
6.5	470± 21		2.34±.061
7.5	121±9.9		2.19±.099
8.5	26.3 ±4.4		2.01±.186
9.5	7.22±2.07		2.29±.393
		23.7	
	C		p_0
4.5	9006±250		2.25±.055
5.5	2648± 79		2.41±.044
6.5	842± 30		2.60±.055
7.5	326± 16		2.59±.068
8.5	104±8.0		2.53±.097
9.5	70.5±5.5		2.65±.111
10.5	19.3±3.0		2.65±.247
		27.3	
	C		p_0
4.5	10310±419		2.62±.095
5.5	2887± 55		2.70±.035
6.5	1058± 25		2.74±.036
7.5	386± 13		2.86±.050
8.5	163±6.4		2.78±.058
9.5	130±5.6		3.10±.075
10.5	41.8±3.1		2.83±.112
11.5	10.2±1.9		2.21±.202

[a] $E\cdot(d^3\sigma/dp^3)=C(1+(p_T/p_0)^2)^{-6}$

[b] Significant data extend to about 3 GeV/c in p_T. See Kaplan *et al.* (ref. 5c).

A High Statistics Study
of Dimuon Production by 400 GeV/c Protons*

S. Childress[1], D. Garelick[2], P. Gauthier[2], M. Glaubman[2],
H.R. Gustafson[3], H. Johnstad[2], L. Jones[3], M. Longo[3], M. Mallary[2],
P. Mockett[1], J. Moromisato[2], W. Oliver[4], T. Roberts[3],
J. Rutherfoord[1], S. Smith[1], E. von Goeler[2], M. Whalley[3],
R. Weinstein[2], and R. Williams[1]

Washington-Northeastern-Michigan-Tufts Collaboration

Fig. 6.

ISR Dileptons. We now have contributions from the ISR where the intrinsically low luminosity is compensated by the very high energy, providing an essential lever arm for studying s-behavior. *The CCOR group* (Fig. 8) has a superconducting solenoid with drift chambers inside and lead glass shower spectrometer outside. They operate in the low β section of the ISR with twice the average luminosity. The data as presented by L. Camilleri has a hardware threshold at ~ 5 GeV and is given in Fig. 9. One sees continuum events and a very clear Υ peak. *The ABCSY*

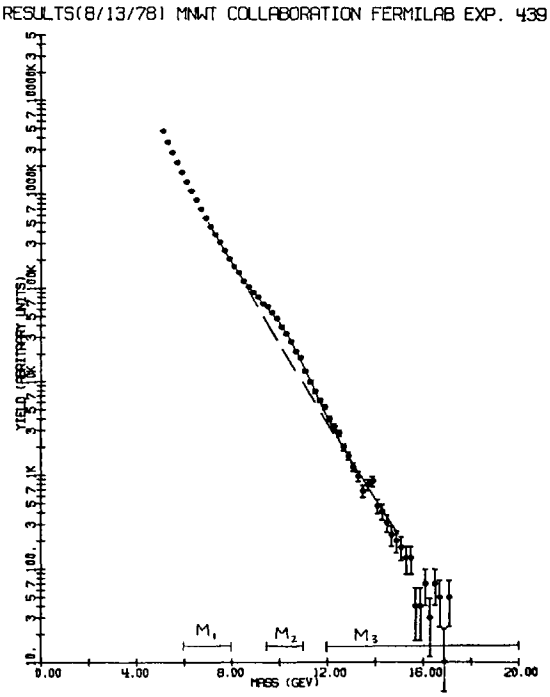

Fig. 7a. SNMT dimuon data 400 GeV protons at FNAL.

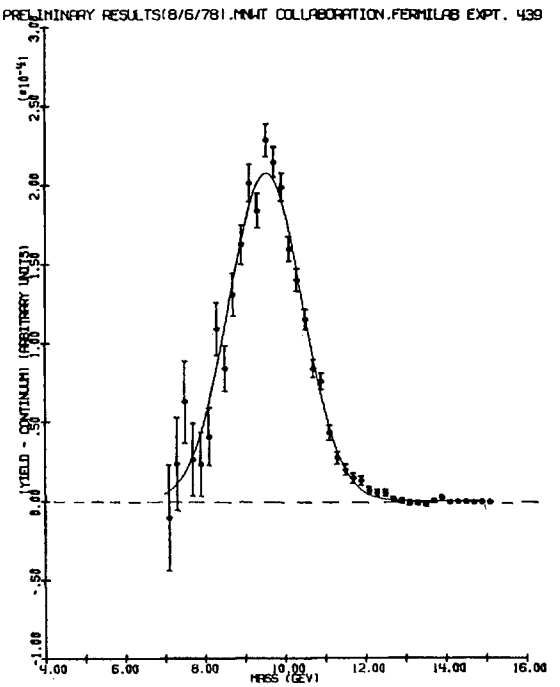

Fig. 7b. SNMT upsilon peak, continuum subtracted.

A Study of High Mass e^+e^- Pairs produced in p-p Collisions
at the CERN ISR

CERN[1]-Columbia[2]-Oxford[3]-Rockefeller[4] (CCOR) Collaboration

A.L.S. Angelis[3], B.J. Blumenfeld[2], L. Camilleri[1], T.J. Chapin[4],
R.L. Cool[4], C. del Papa[1], L. Di Lella[1], Z. Dimčovski[4],
R.J. Hollebeek[2], D. Levinthal[2], L.M. Lederman[2], J.T. Linnemann[4],
L. Lyons[3], N. Phinney[3], B.G. Pope[1*], S.H. Pordes[1], A.F. Rothenberg[4**],
A.M. Segar[3], J. Singh-Sidhu[1], A.M. Smith[1], M.J. Tannenbaum[4],
R.A. Vidal[2***], J. Wallace-Hadrill[3], T.O. White[3†] and J.M. Yelton[3].

Fig. 8.

(*Fig. 10*) data were presented by I. Mannelli as in Fig. 11. This is a detector based upon liquid argon calorimetry with transition radiation to help select electrons. What is dramatic here is the valley just before the Υ peak. Note that the previous two experiments see Υ in its e^+e^- mode. Comparison with CFS *via* scaling or with what follows is a (so far) crude test of μ–e universality in the timelike sector at $Q^2 \sim 100$ GeV^2. *The CHFMNP* (*Fig. 12*) data were presented by H. Newman (Fig. 13). This

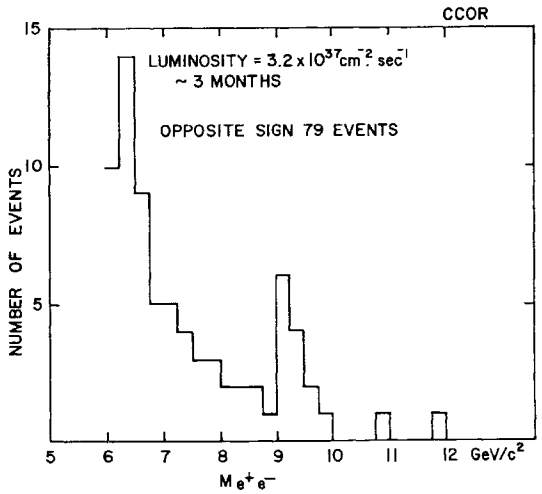

Fig. 9. CCOR electron pair data at $\sqrt{s} = 62$ GeV (ISR).

ABCSY Group

ELECTRON PAIRS PRODUCTION AT THE ISR

C. Kourkoumelis and L.K. Resvanis
University of Athens, Athens, Greece

T.A. Filippas, E. Fokitis
National Technical University, Athens, Greece

A.M. Cnops, J.H. Cobb[6], S. Iwata[1], R.B. Palmer, D.C. Rahm, P. Rehak, S.D. Smith and I. Stumer
Brookhaven National Laboratory[2], Upton, New York 11973, USA

C.W. Fabjan, T. Fields[3], E. Fowler[9], I. Mannelli[4], P. Mouzourakis, K. Nakamura[5], A. Nappi[4] and W.J. Willis
CERN, Geneva, Switzerland

M. Goldberg
Syracuse University[7], Syracuse, New York 13210, USA

and

A.J. Lankford[8]
Yale University, New Haven, Connecticut 06520, USA.

Fig. 10.

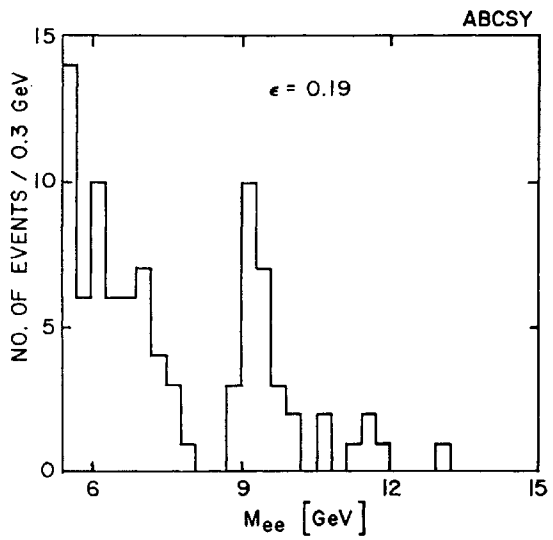

Fig. 11. ABCSY dielectron data at ISR.

CHFMNP Group

MEASUREMENT OF HIGH-MASS MUON PAIRS AT VERY HIGH ENERGIES

D. Antreasyan, W. Atwood, V. Balakin, U. Becker, G. Bellettini, P.L. Braccini, J.G. Branson, J. Burger, F. Carbonara, R. Carrara, R. Castaldi, V. Cavasinni, F. Cervelli, M. Chen, G. Chiefara, T. Del Prete, E. Drago, M. Modous, T. Lagerlund, P. Laurelli, O. Leistam, R. Little, P.D. Luckey, M.M. Massai, T. Matsuda, L. Merola, M. Morganti, M. Napolitano, H. Newman, D. Novikoff, L. Perasso, K. Reibel, J.P.Revol, R. Rinzivillo, G. Sanguinetti, C. Sciacca, P. Spillantini, K. Strauch, S. Sugimoto, S.C.C. Ting, M. Toki, M. Valdata-Nappi, C. Vannini, F. Vannucci, F. Visco and S.L. Wu

(CERN-Harvard-Frascati-MIT-Naples-Pisa Collaboration)

Fig. 12.

detector has large iron toroids and is sensitive to $\mu^+\mu^-$ pairs. This is the largest aperture detector (Table Ib) and has the largest number of events but with the poorest resolution resulting from coulomb scattering in iron.

We put these data together in Fig. 14 to

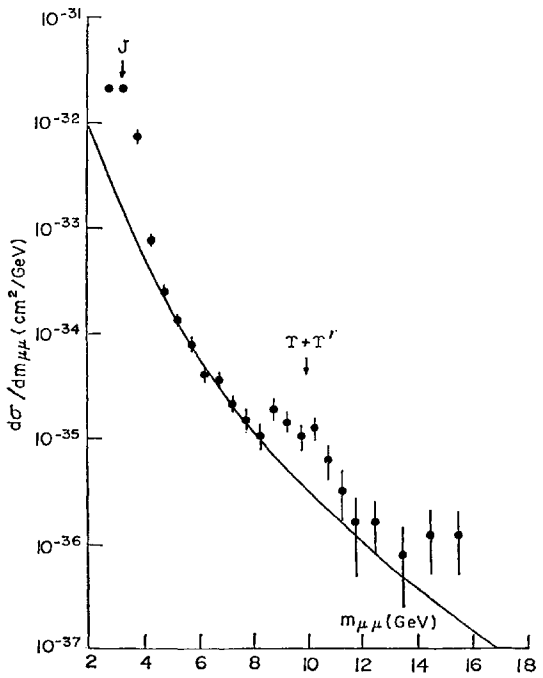

Fig. 13. CHFMNP dimuon data at ISR ($\sqrt{s} = 62$ GeV).

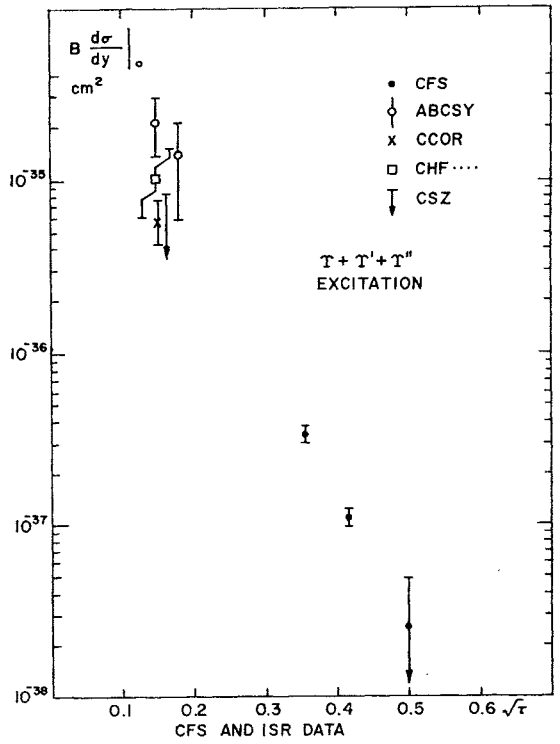

Fig. 14. Upsilon excitation curve.

obtain an excitation curve of Υ production. We are plotting $B(\mathrm{d}\sigma/\mathrm{d}y)|_0$. I have added an upper limit point from CERN–Saclay–Zürich group which was presented by M. Banner. There is some mild controversy. If we overlay a continuum scaling curve (which will be discussed later), one finds that it gives a rough agreement in slope although there is evidence that the continuum levels off whereas the resonance production continues to climb as $m/\sqrt{s}$ decreases. We now summarize upsilon physics:

1. There are three vector mesons at 9.46, 10.02, and 10.4 GeV. In hadron production at $\sqrt{s}=27$ GeV, $B(\mathrm{d}\sigma/\mathrm{d}y)|_0$ ratios are as 1 : 0.3 : 0.15. An early paper of Ellis *et al.*[7] predicted 1 : 0.3 : 0.12 just after the upsilon discovery. This was under the assumption that $\Upsilon=Q\bar{Q}$ (bound state) and $e_Q=-1/3$, in agreement with the recent DESY results,[6] *i.e.* $Q=b$ (beauty or bottom).

2. The upsilon excitation curve behaves roughly like $e^{-20\sqrt{\tau}}$.

3. The Υ'–Υ splitting is sensitive to the details of the $b\bar{b}$ force but it is clear that it cannot be very different from the $c\bar{c}$ force.

4. The ratio of upsilon production to continuum at 400 GeV is 1.26 GeV. At the ISR (3800 GeV), it increases to 4–6 GeV.

5. The CFS group has also determined that the b-quark, bound to u, d cannot be stable.[7a]

§III. Search for New (and Old) Bumps

The CFS experiment, in its e^+e^- phase with $\Delta m/m \sim 1\,\%$ at 400 GeV reported[8] an interesting activity near 6 GeV. Now they have looked carefully at the high resolution dimuon data. See Fig. 15. The ψ' is confirmed but every-

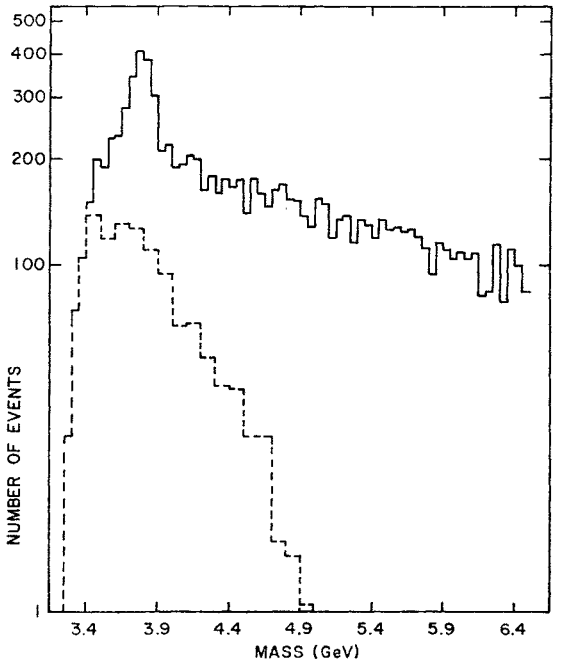

Fig. 15. CFS high resolution data with expanded low mass region. Dashed curve is like sign background.

thing else looks absolutely smooth. In the high mass region, Fig. 4 shows the CFS high intensity data with two events at 19.5 GeV. The continuum fit is also shown. We see only the traditional "bump" that universally appears at the data endpoint. See also Fig. 13. I have two comments: i) In CFS old data, our endpoint was 10 GeV and sure enough, the last data point was high! ii) A paper submitted by Mori, Muraki and Nakagawa to this Conference on logarithmic mass scaling predicts the next quarkonium level at precisely 19.5 GeV!!

Figure 16 shows a dimuon mass spectrum initiated by 225 GeV *pion* reactions at Fermilab presented by Anderson for the CIP group (Fig. 17). Here again, no bumps. The failure to observe Υ may very well be due to the low energy—CFS do not see upsilon at 200 GeV.

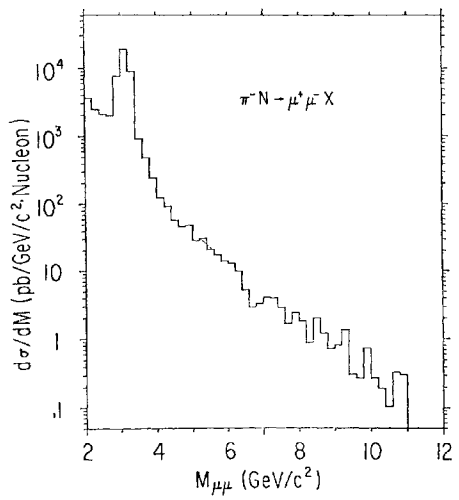

Fig. 16. CIP dimuon data using 225 GeV pions at FNAL.

CIP Group

Hadronic Production of High-Mass Muon Pairs and the Measurement of the Pion Structure Function*

K.J. Anderson, R.N. Coleman, K.P. Karhi, C.B. Newman, J.E. Pilcher, and E.I. Rosenberg

Enrico Fermi Institute, University of Chicago, Chicago, Illinois 60637 U.S.A.

J. J. Thaler

University of Illinois, Department of Physics, Urbana, Illinois, 61801 U.S.A.

and

G. E. Hogan, K.T. McDonald, G.H. Sanders†, and A.J.S. Smith

Joseph Henry Laboratories, Princeton University, Princeton, New Jersey 08540 U.S.A.

Fig. 17.

To quantify the absence of enhancements for $m>11$ GeV, we use the CFS data and assume quite generally that a 4σ resonance would have been claimed. Thus we can set limits according to the following:

mass	14.5	15.5	17	$\geq$18 GeV
upper limit $B(\mathrm{d}\sigma/\mathrm{d}y)\|_0$ $\times 10^{+40}$	10	6	4	1 cm^2

Finally we can discuss the specific case of a $Q\bar{Q}$ state where $e_Q=2/3$, *i.e.*, t-quark (top or truth). Here a specific limit can be placed on the mass of the t-quark if we accept a scaling theorem, *e.g.*, that of Gaisser, Halzen, and Paschos[9] or Ellis *et al.*[7] They propose:

$$\sigma B(t\bar{t})/\sigma B(\Upsilon)=(M_\Upsilon/M_{t\bar{t}})^3\cdot F(\tau)_{t\bar{t}}/F(\tau)_\Upsilon \cdot \Gamma_{\mu\mu}{}^{t\bar{t}}/\Gamma_{\mu\mu\Upsilon} \text{ and } \Gamma_{\mu\mu}/e_Q^2 \text{ scaling,}$$

a form that fits ρ, ϕ, ψ, Υ production. From this, we constructed the following table:

$M(t\bar{t})$	Expected σB	90% Confidence Limit
14	$\sim 7.0\times 10^{-39}$	$\leq 10^{-39}$
16	1.0×10^{-39}	$\leq 5\times 10^{-40}$
18	9×10^{-41}	$<10^{-40}$

On these assumptions, we can conclude that:

$$M_t \geq 7.5 \text{ GeV}.$$

we can also set a limit for $q\bar{q}$ state with $e_q=1/3$:

$$M_q \geq 6.5 \text{ GeV}.$$

§IV. Dilepton Continuum Physics

A. Comments on Drell–Yan analysis

Early in the history of this subject, soon after the 1968 BNL data[4] appeared, Drell and Yan[10] proposed a model for the production of virtual photons: the now famous parton-antiparton annihilation model. In the very widespread application of this model, the parton is a valence quark from one of the colliding nucleons and the anti-parton was an anti-quark from the "sea." The diagram is shown in Fig. 18. Annihilation kinematics

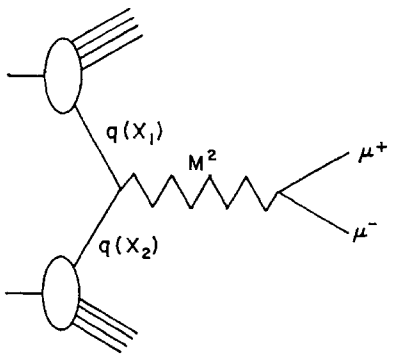

Fig. 18. Drell–Yan process.

yields:

$$x_1x_2=(m^2/s)\equiv\tau \quad x_1=\sqrt{\tau}e^y$$

and

$$x_1-x_2=x_F \qquad x_2=\sqrt{\tau}\,e^{-y}. \tag{1}$$

The D–Y *model* enables one to express the dilepton spectrum as a factored product of a quark (valence) distribution and an anti-quark (sea) distribution:

$$\sigma\sim\sum q(x_1)\bar{q}(x_2)+(x_1\rightleftarrows x_2) \tag{2}$$

e.g. in the case $x_F\cong 0$, $x_1=x_2\equiv x=\sqrt{\tau}$ and:

$$\mathrm{d}^2\sigma/\mathrm{d}m\mathrm{d}y|_0=8\pi\alpha^2/3\cdot 3m^3\times S(x)[\nu W_2^{ep}(x)+\nu W_2^{en}(x)]. \tag{3}$$

Note that one of the factors of "3" in the denominator of the RHS comes from the color degree of freedom. Note also that in (3), we have substituted the inelastic electron proton and electron neutron structure functions for

the valence quark distributions. In the above, we have assumed an SU_3 symmetric sea:

$$\bar{u}(x)=\bar{d}(x)=s(x)\equiv S(x). \qquad (4)$$

The model has a logical series of necessary prerequisites:

1. The collisions must be *hard.*
2. Scaling is implied: At fixed y, $m^3\,\mathrm{d}\sigma/\mathrm{d}m$ depends only on τ.

B. Experimental results

We now look at the data.

1. *Hard collisions* are strongly indicated by the behavior of $\mathrm{d}\sigma/\mathrm{d}m$ with the atomic number A^α. Figure 19 from CFS and Fig. 20 from CIP

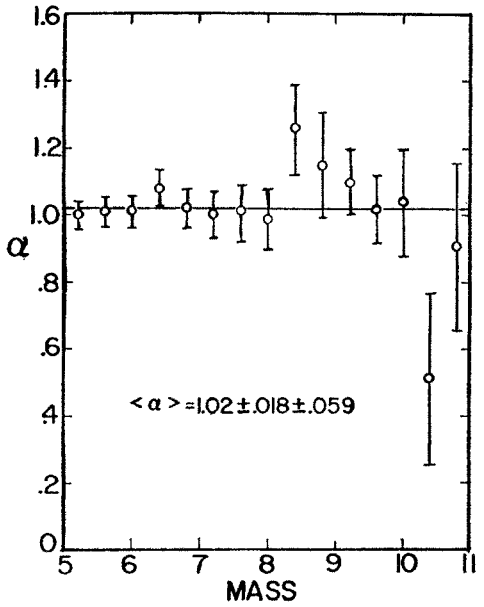

Fig. 19. CFS data on α *vs* $M_{\mu\mu}$ where $\sigma\sim A^\alpha$.

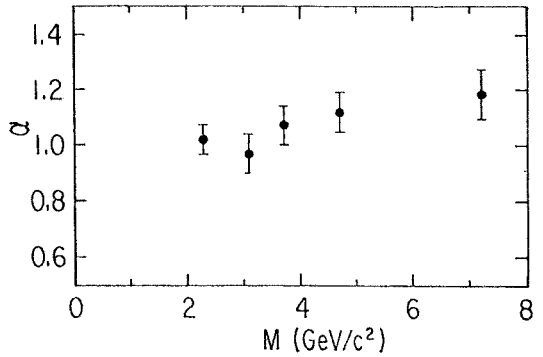

Fig. 20. CIP data on A-dependence (225 GeV pions).

show that $\alpha=1$ for sufficiently massive dileptons in both proton and pion-induced collisions. Here we ignore the possibility that α can exceed unity.

2. *Scaling* has recently been tested by CFS.[5d] Their data taken at 200 GeV, 300 GeV and 400 GeV are shown in Fig. 21. When the data are plotted in dimensionless form,

$$m^3(\mathrm{d}^2\sigma/\mathrm{d}m\mathrm{d}y) \quad \text{or} \quad s(\mathrm{d}^2\sigma/\mathrm{d}\sqrt{\tau}\mathrm{d}y),$$

we find (Fig. 22) that all three energies coalesce to a curve which depends only on τ. Even the old BNL data[4] fit on this universal curve to better than a factor two. The crucial question is whether this form which, at FNAL, spans a small interval of s is still valid at ISR where $E=2000$ GeV, $\sqrt{s}=62$ GeV. For earlier results, see ref. 11.

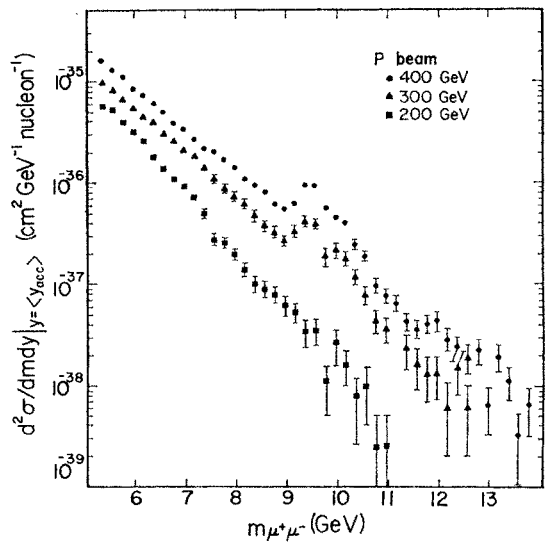

Fig. 21. CFS dimuon spectra at various energies.

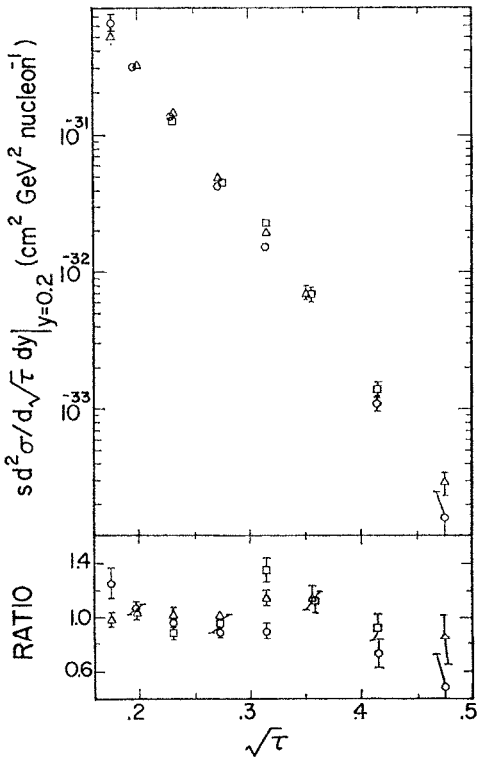

Fig. 22. CFS scaling plot.

Figure 23 presents the analytical "fit" to the CFS universal curve and the ISR data.

Conclusions. The scaling fit for pN collisions:

$$s(d^2\sigma/d\sqrt{\tau}dy)|_0=44.4e^{-26.6\sqrt{\tau}}\mu b \qquad (5)$$

is valid over $0.1\leq\sqrt{\tau}\leq 0.6$; $50\leq s\leq 3800$ GeV^2. The "validity" is at the level of the $\pm 20\%$ normalization errors. These are sufficient to mask the scaling violations we now know should be there at $\sqrt{\tau}>0.2$. There is evidence that for $\sqrt{\tau}<0.1$, the yields exceed the Drell–Yan predictions and probably indicate some other mechanisms. In the case of pion-induced data, we have contributions from CIP (225 GeV), SISI (150 GeV) and Rochester–NSF–BNL (16 and 22 GeV). These do not show scaling behavior but some of the data are preliminary and so I will not dwell on this here.

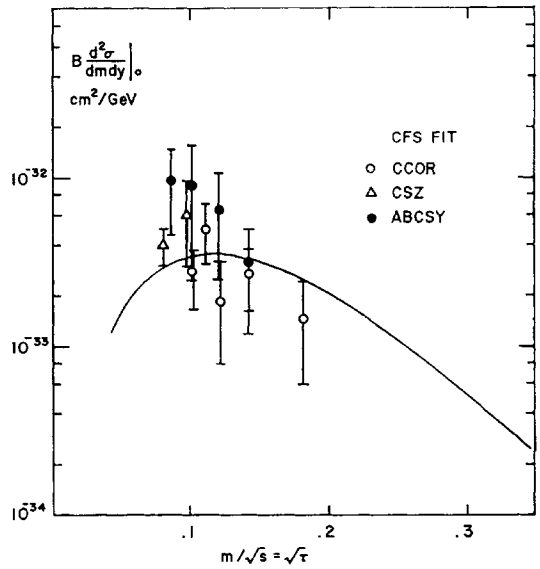

Fig. 23. Confrontation of CFS ($\sqrt{s}=19\to 27$) scaling fit with ISR electron pair data ($\sqrt{s}=63$).

C. *Applications of Drell–Yan analysis*

1. *Sea distributions*

Having satisfied the prerequisites, we now apply the model in a "natural" way:

1. We substitute for the νW_2 terms the *data* on deeply inelastic electron and muon scattering—mainly the newer results from FNAL.[12] Here we note that νW_2 depends on x *and* Q^2 and we set $|Q^2|=m^2$. Figure 24 shows the input data for the valence distributions.

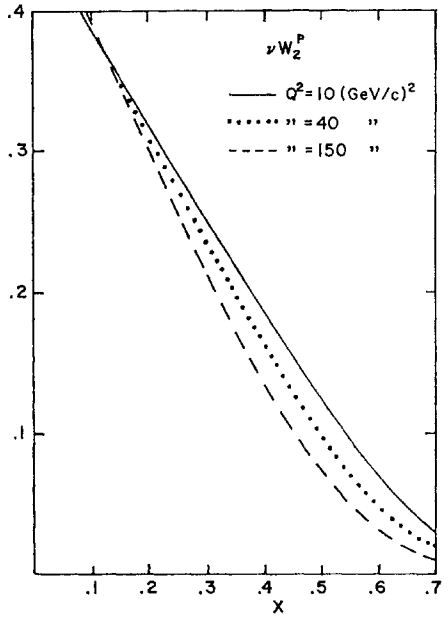

Fig. 24. Fits to FNAL muon scattering data.

2. We use the CFS dimuon spectra (Figs. 16, 21) to derive a sea distribution.

3. We then compare this with ν, $\bar{\nu}$ scattering data (BEBC, CDHS) in order to test the overall consistency.

All of this used to be called the Drell–Yan model. Then it became the *naive* D–Y model. Now, I believe, it is called naive QCD theory and it may well be called naive general relativity before we are through.

In the CFS 400 GeV data[5c] the application of $\nu W_2[x, Q^2=10\ (\mathrm{GeV}/c)^2]$ to eq. (3) gave:

$$S(x)=0.6\,(1-x)^{10}.$$

However, when scale breaking data, $\nu W_2(x, Q^2)$ were installed, they derived a result:

$$S(x)=0.5\,(1-x)^9$$

due to the fact that, at high Q^2, νW_2 falls more rapidly with x. Now with most recent νW_2 data from Fermilab[12] and the $y\neq 0$ data from CFS, we find the following results for the sea:

$$\text{Set}\quad \bar{d}=A(1-x)^n$$
$$\bar{u}=\bar{d}(1-x)^\alpha$$
$$\bar{s}=\bar{d}(1-x)^\beta$$

Trial	A	n	α	β	χ^2/DF
SU(3) (eq. 4)	0.54±0.02	8.5±0.1	0	0	237/181
Field–Feynman[13]	0.57±0.02	7.4±0.1	3	1	214/181
Free	0.56±0.02	7.5±0.15	2.6±0.6	1.5±4	213/179

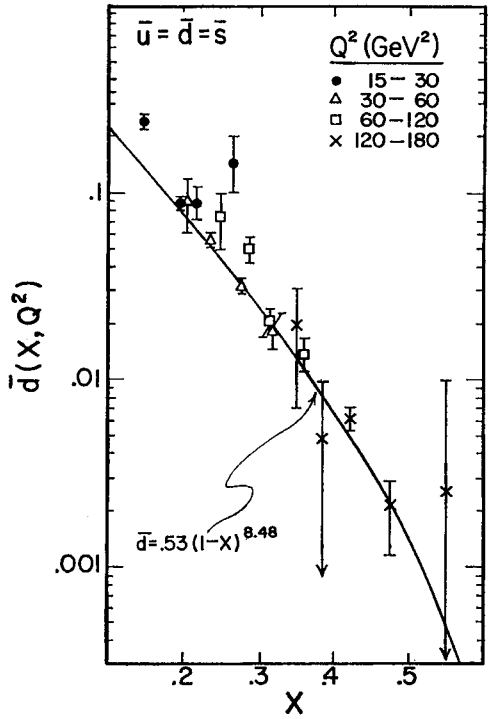

Fig. 25. Sea distribution fit from CFS data.

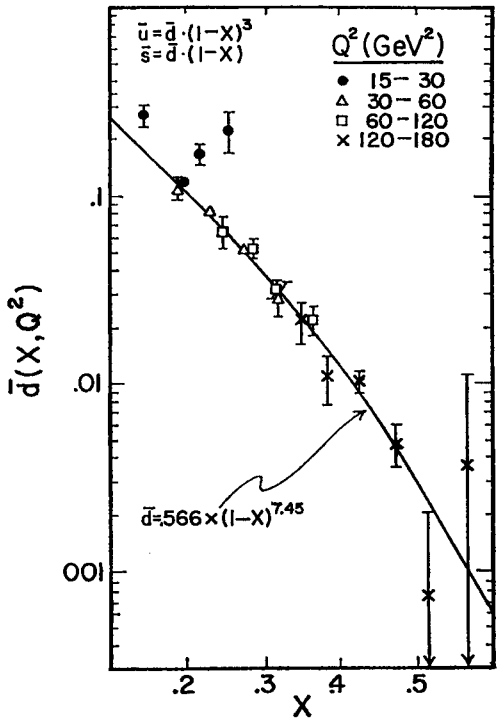

Fig. 26. Sea distribution from CFS data with $\bar{u} \neq \bar{d}$.

Thus the data favor an SU(3) asymmetric sea along the lines of a speculation by Field and Feynman[13] that the $\bar{u}$ content of the proton sea would be Pauli inhibited by the larger u content in the valence cloud.

Figure 25 shows the SU(3) symmetric fitted curve for $\bar{d}(x, Q^2)$ and our experimental points. Figure 26 shows the more favored solution.

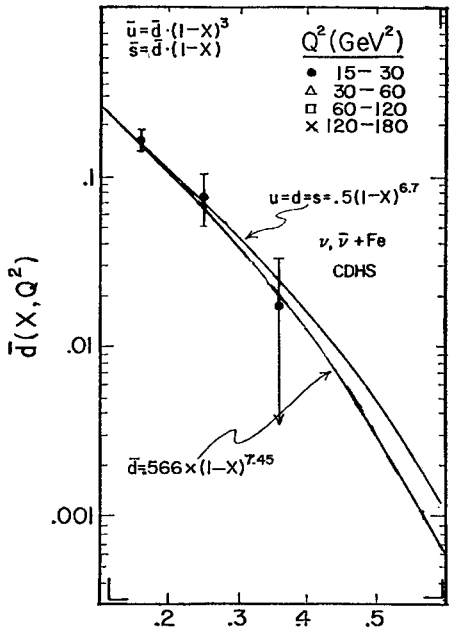

Fig. 27. Comparison of CFS dimuon sea fit with CHDS neutrino scattering fit from K. Tittel, this Conference.

Note that although there is no evidence for strong Q^2 dependence, the large x region is dominated by high Q^2 data only. Now the most exciting result at this conference, I find, is the comparison of our sea fit (Fig. 26) with the CDHS data as shown in Fig. 27. We note the agreement:

CFS (dimuons)

$$\bar{d}(x)=(0.56\pm0.02)(1-x)^{7.5\pm0.15}$$

CDHS (ν, $\bar{\nu}$ scattering)

$$\bar{d}(x)=0.5(1-x)^{6.7\pm0.5}$$

CERN data from BEBC are consistent with these forms.

We conclude:

1. The D–Y model or its QCD version now permits a parameter free prediction of the reaction:

$$p+N\rightarrow\mu^+ +\mu^- +\text{anything}$$

using as input, the data on

$$e,\ \mu^{\pm}+N\rightarrow\mu^{\pm}+\text{anything}$$

and

$$\nu,\ \bar{\nu}+N\rightarrow\mu^{\pm}+\text{anything}.$$

We believe this to be a remarkable achievement.

2. The color factor of "3" is required.

3. There is evidence that the sea is not SU (3) symmetric, a prediction by Field and Feynman.

2. *Rapidity distribution*

The FNAL CFS data have a rather narrow y-acceptance which moves with incident energy (Fig. 28). Under the scaling hypothesis, this permits a respectable coverage in y. Figure 29 shows that the three energies combine to give a smooth picture of the y-behavior. If we calculate the slope of the y-distribution at $y=0$, we have a new test of the D–Y model presented in Fig. 30. The solid line is the D–Y model predictions obtained from the $y=0$ data at 400 GeV. The agreement in sign of the slope, magnitude and behavior with $\sqrt{\tau}$ is another success of the model. The agreement becomes even better if we let $\bar{d}\neq\bar{u}$. The data of SNMT against x_F indicates the same asymmetric behavior around $x_F=0$.

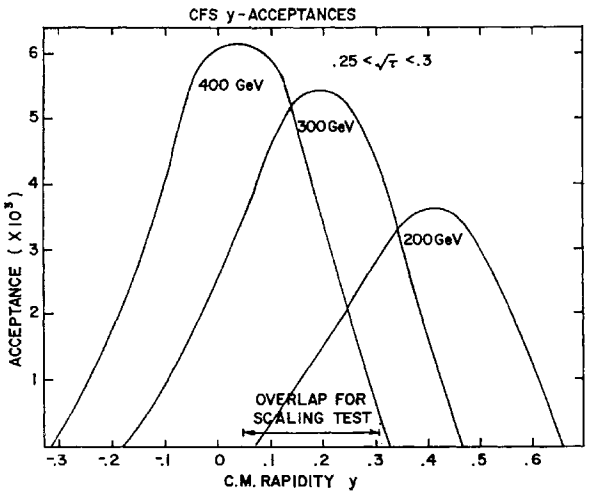

Fig. 28. CFS rapidity acceptances.

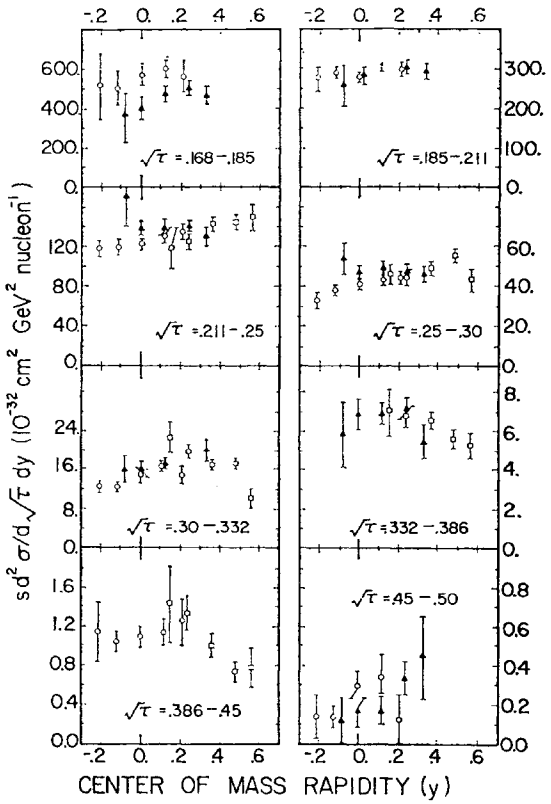

Fig. 29. CFS y-behavior.

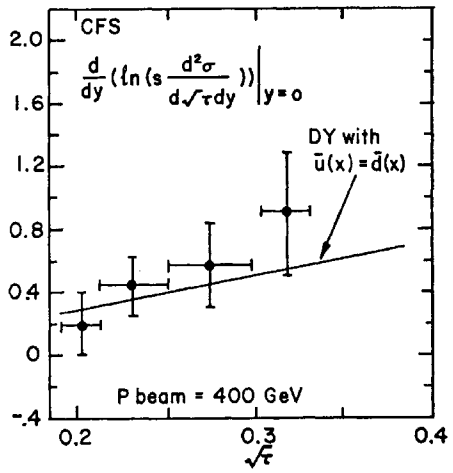

Fig. 30. Asymmetry behavior of CFS data *vs* $m/\sqrt{s}$.

3. *Pion-induced dimuons*

The CIP data (Fig. 16) have been analyzed to extract pion structure functions. This is a forward spectrometer based upon a large air magnet which was once the Chicago cyclotron.

In contrast with the proton collisions, pions bring in a valence anti-quark. High masses should be easier to make since one does not need the sea to obtain $q(x_1)\bar{q}(x_2)$ annihilations with large product x_1x_2. This is qualitatively seen in the mass spectrum of Fig. 16.

The π induced mass spectrum is written by CIP as:

$$d^2\sigma/dm\,dx_F = 8\pi\alpha^2/9m^3(1/(x_1+x_2))\, f_\pi(x_1)f_N(x_2) \qquad (6)$$

and if variables are changed according to eq. (1):

$$d^2\sigma/dx_1dx_2 = 4\pi\alpha^2/9\cdot s\cdot f_\pi(x_1)f_N(x_2). \qquad (7)$$

Here $f_\pi(x)=x\bar{u}^\pi(x)$; $f_N(x)=4/9xu^N(x)+1/9x\bar{d}^N(x)$. Their first test is that of the factorizing prediction of the D–Y model, *i.e.*, that the cross section may be written as a function of x_1 times a function of x_2. They obtain a fair χ^2 for this hypothesis and then go on to fit the two functions in eq. (7): Figs. 31, 32 give their results. A form $(1-x)^a$ with $a=1$ is predicted by quark counting rules of Brodsky and Farrar. However, the nucleon function derived from

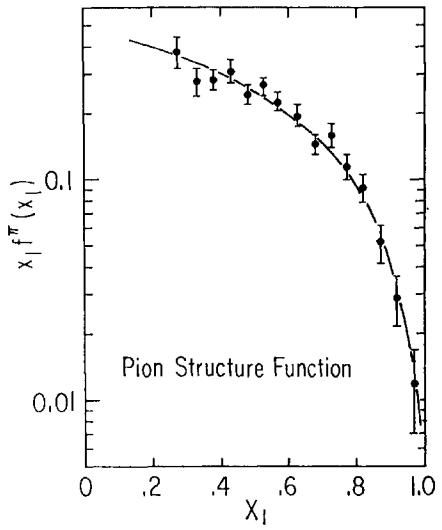

Fig. 31. CIP pion structure function from 225 GeV π^- dimuons.

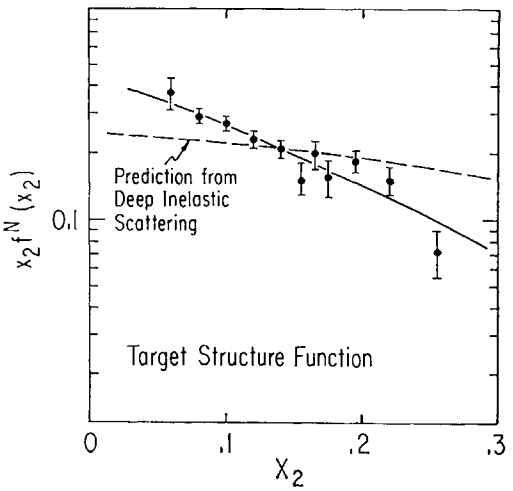

Fig. 32. CIP nucleon structure function.

CIP data is not in good agreement with muon scattering. The authors note that this *may* be related to the fact that the p_T of the muon pair has been neglected in the D–Y analysis and thus, at the least, affects the definitions of x_1 and x_2. A model for including the kinematic effects of p_T of the quarks seems to be in the right direction of flattening the nucleon structure function. The analysis is continuing but it is clear that the correct nucleon structure must be acceptable if the pion structure is to be convincing.

In summary, the first data on the quark distributions in the pion are given: $xu^\pi(x) = 0.27(1-x)^{1.05}$ ($x>0.25$). The data also imply that half the pion momentum is carried by gluons.

4. *Further Tests of the D–Y Model*

i. π^+/π^- *ratio in carbon.*

This is a famous test implied by the fact that a π^+ furnishes a $\bar{d}$ valence quark to a nucleon system symmetric in u and d receptors. The π^- supplies a $\bar{u}$ and therefore the ratio of cross sections should simply be the square of the ratio of the $\bar{d}$ to $\bar{u}$ charges, *i.e.*, 1 : 4. This neglects the seas in both pions and nucleons and so one expects to approach 0.25 as the dilepton mass increases. Figure 33 shows the CIP data. More success! Earlier data from CERN confirm this result.[14]

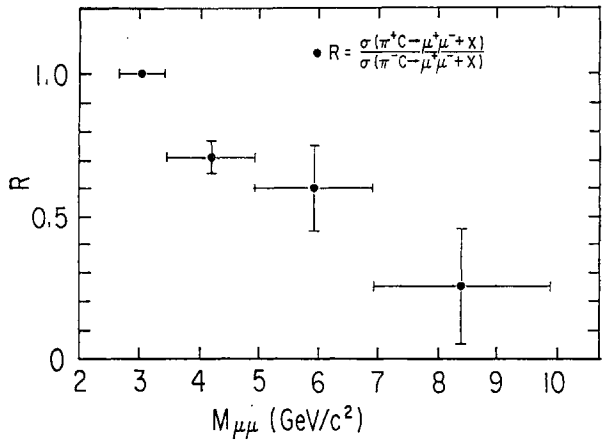

Fig. 33. CIP π^+/π^- data.

ii. *Helicity angular distributions*

The D–Y model for the annihilation of two spin 1/2 quarks into a 1^- state predicts a distribution

$$f(Q) = 1 + \alpha \cos^2 \theta^*; \quad \alpha = 1 \qquad (8)$$

where θ^* is the angle between the outgoing back-to-back muons and the collision axis in the dimuon rest frame. This picture is made vastly more complicated if the quarks have transverse momenta because then the collision axis is unknown. Figure 34 shows CIP data for π induced dimuons restricted to $p_T < 1$ GeV/c and they find $\alpha = 1$ for these data and, in fact $\alpha > 1$ for data which include all p_T. The SNMT group can also fit their data to the form (eq. (8)) and also find strong alignment, $\alpha > 1$. We view the small p_T data as being a clear success of the model and guess that the large values of α are a result of some complicated interaction between θ^* and p_T acceptances since most effects would tend to decrease α.[15]

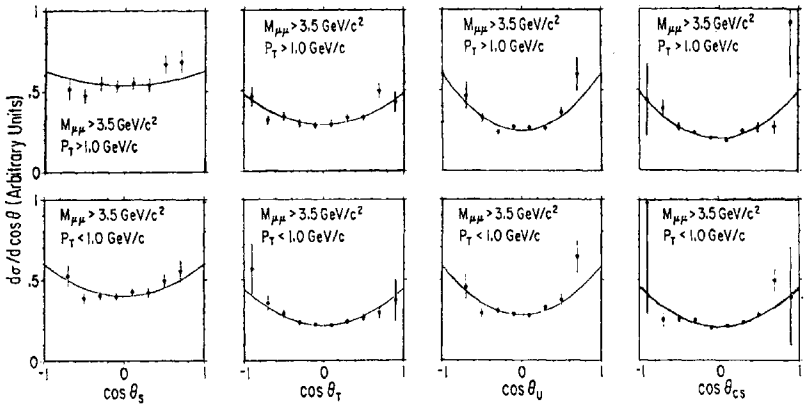

Fig. 34. CIP helicity angle data.

We summarize:

As applied by naive experimentalists, the Drell–Yan model works:

1. The nucleon sea deduced from dilepton production is the same as that deduced from neutrino scattering.
2. Color degree of freedom is observed.
3. The y distributions in p–N and π–N are as predicted.
4. The π^+/π^- production of dileptons in C approaches 0.25 as the mass increases.
5. The helicity distribution is $1+\cos^2\theta^*$.

Furthermore, we have a quantitative ($\sim 20\%$) photograph of the nucleonic quark sea and the pionic valence quark cloud. This success of what appears to be the most simple model is made even more encouraging when we learn that perturbative QCD, a real theory, yields the D–Y model as we have used it, when diagrams involving quarks and gluons are summed to first order in $\alpha_s \log Q^2$. All of this is the good news. We now turn to a more troublesome and therefore more interesting subject.

D. *Dilepton transverse momenta*

If we integrate over p_T as we have done in the preceding (with some anxiety about the kinematic definitions, eq. (1)), we have a very successful model. Our theoretical colleagues patiently explain that what we have done is to apply QCD, summing all first order diagrams involving not only $q\bar{q}$, but qG, GG etc. where G are the gluons, the objects that generate the quark–quark forces. Experimentalists accept this feat modestly but then we observe that dileptons have large transverse momentum. Even the old BNL data[4] observed $\langle p_T\rangle \sim 800$ MeV/c. The model neglected p_T (~ 300 MeV/c was expected). The earliest FNAL experiments[8] observed $\langle p_T\rangle \gtrsim 1$ GeV/c for $m>4$ GeV. Now the fundamental issue is that the dilepton transverse momentum p_T is related to the transverse momentum of the annihilating quarks k_T:

$$p_T = k_{T_1} + k_{T_2}.$$

Constituent transverse momenta are coupled to the deepest aspects of the quark thoery, QCD and therefore it was not surprising that a very large number of theoretical papers addressed this issue (see talks at this Conference by Halzen, Fritzsch, Matsuda, Berger, Field, Politzer, others).

Now the data.

i. p_T *vs* m

CFS finds that, out to ~ 3 GeV/c of dilepton p_T and for $m \gtrsim 5$ GeV, there is an empirical fit (with excellent χ^2):

$$E(d^3\sigma/dp^3) = A(m)[1+p_T^2/p_0^2]^{-6} \qquad (9)$$

where p_0 depends very little on mass but it does depend on energy. Table III lists p_0's. The SNMT group (see Fig. 35) also find this form excellent with very similar p_0's. The confrontation with the QCD diagrams has been made by many papers—I show in Fig. 36 the work of E. Berger presented to this Conference. Typical of these calculations is a p_T^{-2} divergence. Some of the earliest of such calculations were carried out by Politzer,[16] by Altarelli *et al.*[17] who have also tried to improve the low p_T behavior by a regularizing process. The idea is that there are two sources of dilepton p_T: One comes from the QCD gluonic diagrams (the same ones that account for the scale breaking in νW_2), and the other from "intrinsic" p_T related by the uncertainty principle to the fact that quarks are confined in

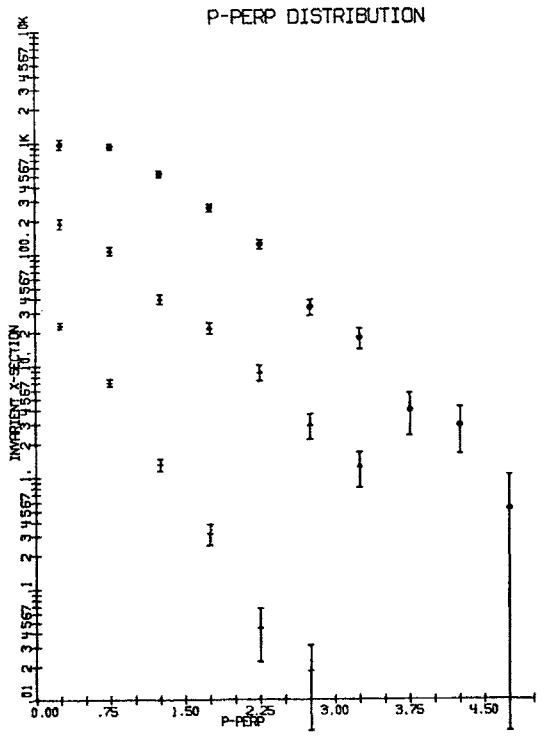

Fig. 35. SNMT dimuon p_T distributions (400 GeV protons at FNAL).

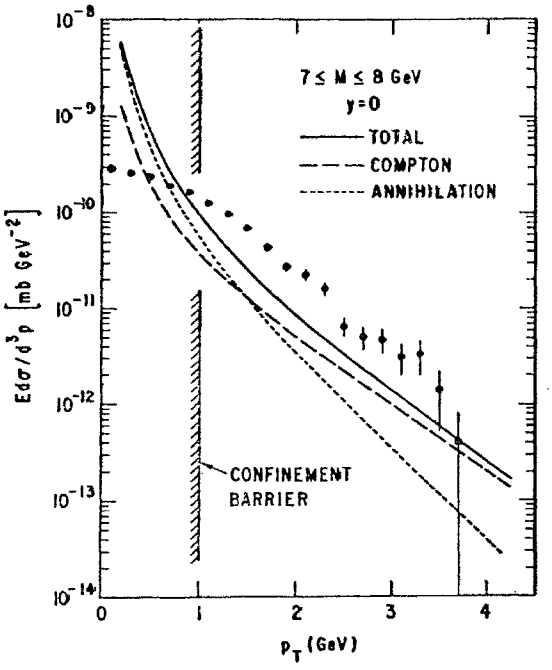

Fig. 36. QCD calculation of dilepton p_T distributions from E. Berger (this Conference).

space.

To study the behavior of p_T with mass, energy, rapidity (or x_F), it is simplest to calculate the moments: $\langle p_T \rangle$ or $\langle p_T^2 \rangle$. Where possible, we also calculate a bizarre $\langle p_T \rangle$ in which we only count $p_T > 1$ GeV (say). We can still explore the variation with m, s etc. to see whether or not the observed behavior is dominated by low p_T.

The CFS data are presented in Fig. 37. We see a flattening of $\langle p_T \rangle$ *vs* mass for $m \geq 5$ GeV (except for the Υ). Figure 38 shows the

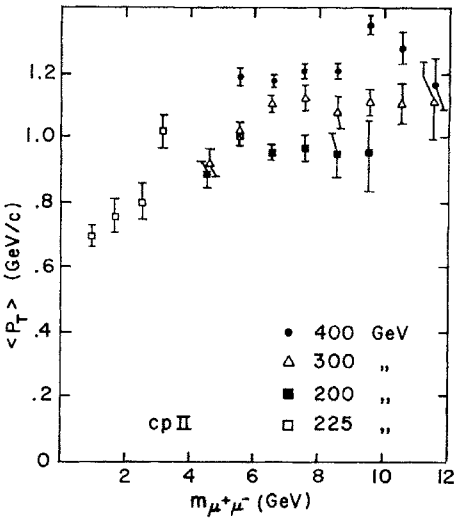

Fig. 37. CFS average p_T *vs* $M_{\mu\mu}$.

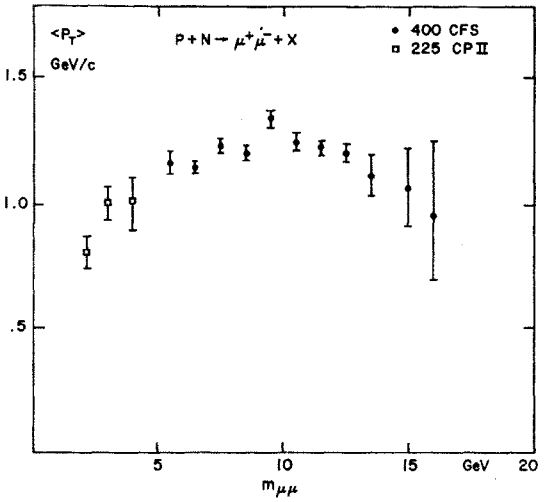

Fig. 38. High intensity CFS $\langle p_T \rangle$ *vs* mass.

increased CFS data sample and a falling off at very high mass is indicated. The SNMT group agrees; this is also seen (see Fig. 39) by the CIP group for pion-induced dileptons. (The flatness persists if we neglect $p_T < 1$ GeV). Here we have a surprise for experimentalists. $\langle p_T \rangle$ of pions is clearly $> \langle p_T \rangle$ of protons. Some theoretical implications: The earliest estimates (*e.g.*, Politzer[16]) indicated that

$$\langle p_T \rangle \sim m^2/\log m^2$$

and this did not happen. The essential parameter in converting the above to the observed flat distribution is the adjustment of the gluon distribution to

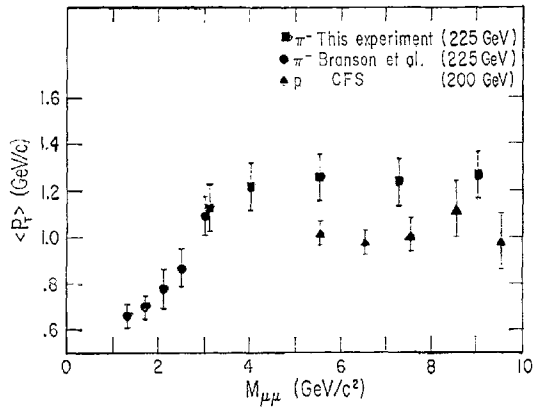

Fig. 39. Comparison of proton and pion-induced $\langle p_T \rangle$ *vs* mass.

$$xG(x) \sim (1-x)^6.$$

Now if we look at the dominant gluon correction diagram for pN collisions it involves quark–gluon collisions to produce quark–virtual photon final states. In the πN case it is quark–antiquark scattering into gluons and virtual photons which dominates. If we now appeal to the hierarchy:

pion valence $\sim(1-x)$—from πN$\rightarrow$dileptons
nucleon valence $\sim(1-x)^3$—from μN scattering
gluons $\sim(1-x)^6$—from dilepton p_T
nucleon sea $(1-x)^8$—from dilepton spectrum. (9)

We see that π(valence) N(valence) collisions are harder than p(valence) G collisions. Since, in these diagrams, p_T arises from the conversion of longitudinal momentum, we understand the higher $\langle p_T \rangle$ for πN.

ii. p_T *vs* x_F *or* y

The same qualitative argument given above suggests that at very large dilepton x_F, the $\langle p_T \rangle$ must decrease since it all derives from initial parton x. The data from CFS, CIP and SNMT are given in Figs. 40 a, b, c. One sees no drop-off and this also persists if $p_T < 1$ GeV is neglected. The predicted fall-off is moderated by the intrinsic p_T if this is independent of x but we leave this as an unsettled question.

iii. p_T *vs* s

Figure 41 presents the CFS data and fit together with a new ISR data point from CCOR for $6 < m < 9$ GeV. This data point has been raised from the observed $\langle p_T \rangle = 1.65$ GeV/c to 1.9 GeV/c in order to make it fit our line but also because at ISR, $\sqrt{\tau} = 0.1$ and we

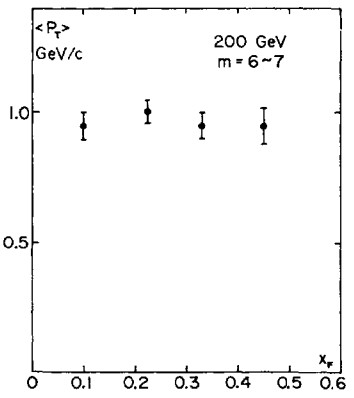

Fig. 40a. CFS $\langle p_T \rangle$ *vs* x_F.

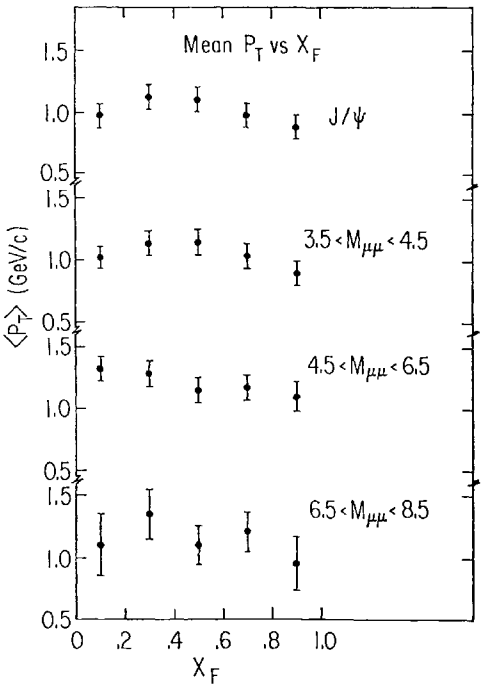

Fig. 40b. $\langle p_T \rangle$ *vs* x_F.

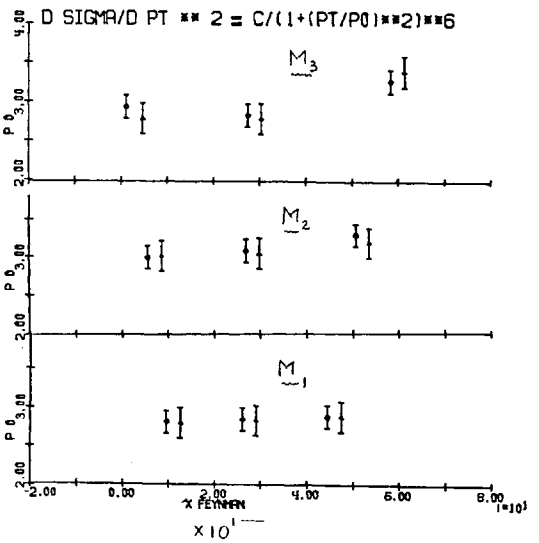

Fig. 40c. SNMT p_0 parameter (eq. 9) *vs* x_F for 3 mass bins.

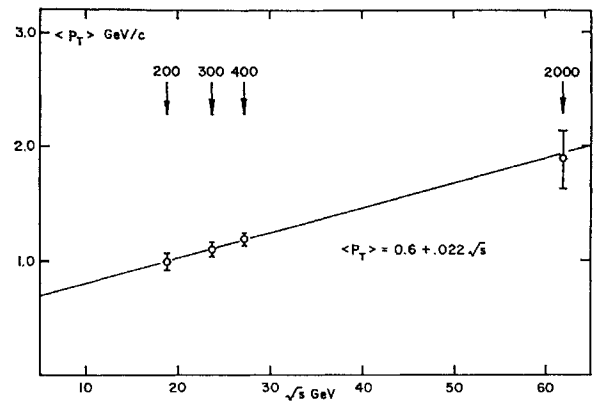

Fig. 41. CFS and CCOR $\langle p_T \rangle$ *vs* $\sqrt{s}$.

know that $\langle p_T \rangle$ increases with $\sqrt{\tau}$ until $\sqrt{\tau} > 0.2$. We used the theoretical papers of Matsuda and also of Fritzsch to make this correction and so we can write

$$\langle p_T \rangle = 0.6 + 0.022 \sqrt{s}\ \text{GeV}/c. \qquad (10)$$

The CFS results are not changed (in slope) if we delete the $p_T < 1$ GeV events. This behavior seems to confirm interpretation in terms of a confinement piece of parton k_T (giving rise to $\langle p_T \rangle \sim 600$ MeV/c) and a dynamical piece which depends on $\sqrt{s}$. It should be pointed out that Fritzsch and Minkowski[18] had published a prediction:

$$\langle p_T \rangle = (0.55 + 0.023 \sqrt{s})\ \text{MeV}/c.$$

So this form is certainly consistent with QCD and clearly illustrates scale breaking. The implied quark k_T is somewhat lower than is obtained from other kinds of analysis.[19]

Final Remarks

Dilepton data have produced crucial tests of the constituent theory. We can now predict the dilepton data completely from lepton-nucleon scattering with no parameters. Our theoretical colleagues have done very well because the collision of two such ugly objects as protons to produce a pair of leptons would offhand look entirely unconnected to the elegant neutrino and electron (muon) scattering. This is a major intellectual achievement (to the level of 20%!). We have also given shape to the pion, and the esoteric gluon cloud and sea of nucleon. They are all enumerated.

Occasionally this study of the property of the old quarks is pleasantly interrupted by a new quark. It is characteristic of the field which must now work hard to improve the precision in the familiar domain and also extend the parameters—certainly to the W with which we began this subject.

References

1. Y. Yamaguchi: Nuovo Cimento **43** (1966) 193.
2. W. Burns *et al.*: Phys. Rev. Letters **15** (1965) 830.
3. L. Okun: Sov. J. Nucl. Phys. **3** (1966) 426.
4. J. Christenson *et al.*: Phys. Rev. Letters **25** (1970) 1523; Phys. Rev. **D8** (1973) 2016.
5. (a) S. Herb *et al.*: Phys. Rev. Letters **39** (1977) 252; (b) W. Innes *et al.*: Phys. Rev. Letters **39** (1977) 1240, 1640E; (c) D. Kaplan *et al.*: Phys. Rev. Letters **40** (1978) 435; (d) J. Yoh *et al.*: Phys. Rev. Letters **44** (1978) 684.
6. Bienlien *et al.* (DESY-Heidelberg): this Conference; Darden *et al.* (DASP II): this Conference.
7. Ellis, Gaillard, Nanopoulos and Rudaz: Nucl. Phys. **B131** (1977) 285; (a) R. Vidal *et al.*: Phys. Letters **77B** (1978) 344. See also D. Cutts *et al.*: Phys. Rev. Letters **41** (1978) 363.
8. D. Hom *et al.*: Phys. Rev. Letters **36** (1976) 1236; Phys. Rev. Letters **37** (1976) 1374.
9. Gaisser, Halzen and Paschos: Phys. Rev. **D15** (1977) 2572.
10. S. Drell and T. M. Yan: Phys. Rev. Letters **25** (1970) 316; Ann. Phys. (N.Y.) **66** (1971) 578.
11. L. Lederman and B. G. Pope: Phys. Letters **66B** (1977) 486; Antreasyan *et al.*: Phys. Rev. Letters **39** (1977) 906.
12. H. Anderson *et al.*: Phys. Rev. Letters **40** (1978) 1061; T. Kirk: private communication.
13. R. Field and R. P. Feynman: Phys. Rev. **D15** (1977) 2590.
14. Cordon *et al.*: Phys. Letters **76B** (1978) 226.
15. E. Berger *et al.*: from ANL–HEP–PR 77–63 (1977).
16. H. D. Politzer: Nucl. Phys. **B129** (1977) 301.
17. G. Altarelli, G. Parisi and R. Petronzio: Phys. Letters **76B** (1978) 351, 356.
18. H. Fritzsch and P. Minkowski: Phys. Letters **73B** (1978) 80.
19. S. Matsuda: KUNS 467 HE(TH) 78/08, and this Conference.

P3a: Dynamics of Hadronic Reactions

Chairman: A. WROBLEWSKI
Speaker: G. VENEZIANO
Scientific Secretaries: N. SAKAI
S. WADA

P3b: Dynamics of High Energy Reactions

Chairman: L. D. SOLOVIEV
Speaker: R. FIELD
Scientific Secretaries: T. MUTA
T. UEMATSU

(Monday, August 28, 1978; 15: 00–16: 00, 16: 20–17: 20)